

# Logarithmic coarsening and glassy behavior in a polymer model with mass-dependent diffusion

F. D. A. Aarão Reis<sup>1,\*</sup> and R. B. Stinchcombe<sup>2,†</sup>

<sup>1</sup> *Instituto de Física, Universidade Federal Fluminense,  
Avenida Litorânea s/n, 24210-340 Niterói RJ, Brazil*

<sup>2</sup> *Rudolf Peierls Centre for Theoretical Physics,  
Oxford University, 1 Keble Road, Oxford OX1 3NP*

(Dated: November 14, 2018)

## Abstract

We present a model of polymer growth and diffusion with frustration mechanisms for density increase and with diffusion rates of Arrhenius form with mass-dependent energy barriers  $\Gamma(m) \sim (m - 1)^\gamma$ . It shows non-universal logarithmic coarsening involving the exponent  $\gamma$ . Strong-glass behavior is found in the typical times for disappearance of all polymers up to a given length, without reference to the equilibrium states of the macroscopic system. These features are predicted by numerical simulations, scaling theories and an analytic solution of the master equation within an independent interval approximation, which also provides the cluster size distribution.

PACS numbers: PACS numbers: 05.50.+q, 05.40.-a, 68.43.Jk

---

\* Email address: reis@if.uff.br

† E-mail address: r.stinchcombe1@physics.ox.ac.uk

## I. INTRODUCTION

One of the most remarkable features of glassy systems is the rapid increase of the relaxation time  $\tau$  to equilibrium states as the temperature  $T$  is lowered. In the most simple glasses, called strong glasses, an Arrhenius behavior  $\tau \sim \exp(A/T)$  is observed, while in fragile glasses more complex temperature-dependences are found. This slow relaxation is expected to be accompanied by a slow growth of correlated domains. Several microscopic models have already been proposed to represent such features [1, 2]. For instance, strong glass behavior was found in the spin-facilitated models introduced by Fredrickson and Andersen [3, 4] and several glassy features were found in models with kinetic constraints [5, 6, 7, 8], in which initial random systems evolve to equilibrium states via the slow diffusion of defects. On the other hand, fragile glass relaxation to equilibrium states with  $\tau \sim \exp(B/T^2)$  was recently shown in a spin chain with asymmetric kinetic constraints [9, 10]. The dynamic rules assumed during the non-equilibrium evolution of these systems are derived from statistical equilibrium conditions. For instance, in the spin-facilitated models, the final concentration of defects is given by the canonical distribution  $\exp(-E/T)$  at low temperatures and this is the origin of the Arrhenius form of the relaxation time in those systems.

An alternative scenario for the onset of anomalous coarsening and glassy behavior is suggested in this paper with the analysis of a polymer growth model in one dimension. The slow dynamics in this model is a consequence of the interplay between slow activated (Arrhenius) diffusion of clusters and frustration of density increase. Cluster diffusion occurs in thermal contact with the surroundings, with energy barriers increasing with cluster length. Density increase is represented by the deposition of new particles in the line, but it is not allowed at small vacancies between the clusters. Thus, the dynamic rules of this model do not make any reference to equilibrium macroscopic states and the physical motivation of those processes contrasts with the somewhat artificial stochastic rules of other simple models with similar dramatic slowing.

The rules of the model, illustrated in Figs. 1a and 1b, prescribe as follows the influence of polymer length on activated diffusion, the suppression of density increase, and the irreversible polymer aggregation. A cluster (polymer) can move one lattice spacing to the right or to the left with diffusion rate given by  $r \equiv \exp(-\Gamma/T)$ , where the energy barrier  $\Gamma$  increases with polymer length and  $T$  is the temperature (Fig. 1a). We will assume that

$\Gamma \sim (m - 1)^\gamma$ , where  $m$  is the polymer length (mass) and  $\gamma > 0$ . Deposition of hard core particles, which represents density increase, is allowed only at sites with one empty nearest neighbor, with deposition rate  $F = 1$  (Fig. 1b). Aggregation of a particle to a cluster and of two clusters is irreversible and occurs upon any contact of nearest neighbors. Thus, after a diffusion event, the most typical situation is the formation of a larger cluster (Fig. 1a). This represents an ideal polymerization process, with no energy barrier for the formation of a new bond between neighboring particles and an infinite barrier for the reverse process. The linear increase of  $\Gamma$  with  $m$  ( $\gamma = 1$ ) would correspond to polymers stretched along a surface, with  $\Gamma$  being the sum of adsorption energies of all monomers. Although not directly related to the present problem, it is also relevant to recall that energy barriers with  $\gamma \approx 0.5$  are found in desorption of linear alkanes from graphite surfaces [11]. Consequently, our numerical study will be concentrated in systems with  $\gamma \sim 1$ .

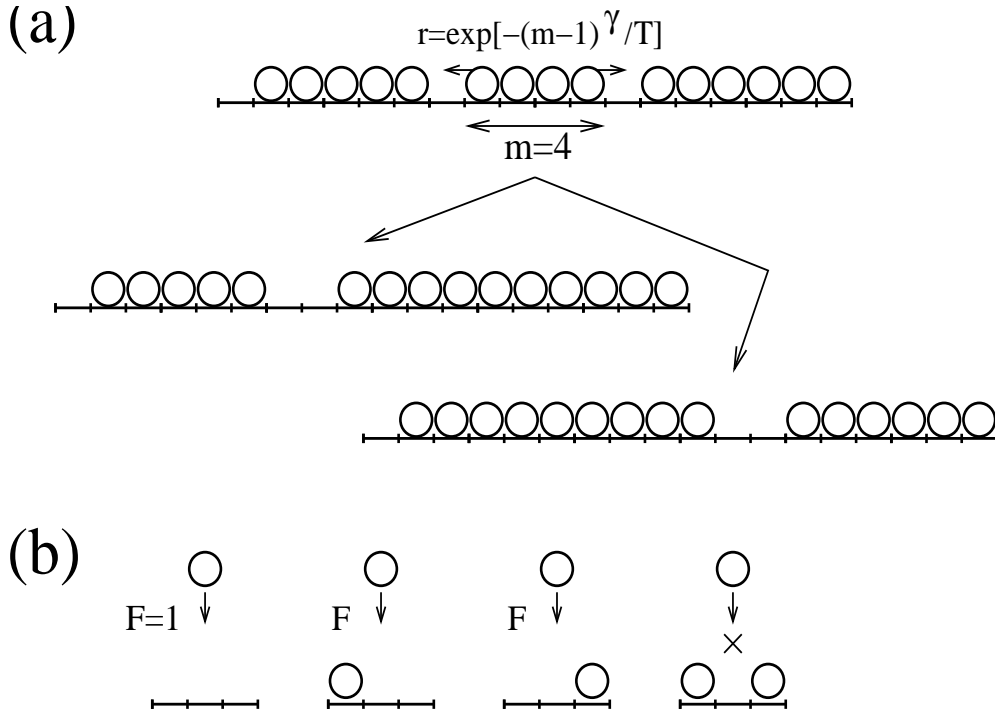


FIG. 1: (a) Diffusion of a polymer of length (mass)  $m$ , with the corresponding rate  $r$ , and the two possible final configurations after the polymer move. (b) Allowed deposition processes at vacancies with a neighboring vacant site, with the corresponding rate, and the forbidden deposition process, in which the vacancy has two occupied neighbors.

The restriction of the model to a low-dimensional structure helps to obtain the analytical

and numerical solutions. This is certainly a simplification for many systems, in which the dimensionality may play an important role. However, glassy behavior has been seen in several low-dimensional systems, such as polymer films [12], and the formation of clusters of fast-moving particles with dimensions near or below 2 was observed in colloidal glasses [13]. Consequently, we believe that the qualitative scenario introduced here may find applications to real systems.

Using scaling arguments and numerical methods, we will show that the model presents non-universal logarithmic coarsening, in which the average cluster (polymer) length slowly increases as  $\langle m \rangle \sim (T \ln t)^{1/\gamma}$ , starting from an initial random low-density configuration. The model also presents strong-glass features of the characteristic times for eliminating structures of a given length: after a time  $\tau \sim \exp[d^\gamma/T]$ , all clusters of sizes of order  $d$  or smaller will disappear. Consequently, the anomalous coarsening and the Arrhenius-type relaxation are observed during the non-equilibrium system evolution, which involves frustration of density increase and thermally activated diffusion at the microscopic level. We will also solve the master equation of the process within an independent interval approximation, using the same mapping onto a column picture adopted in the study of related systems in Refs. [14] and [15]. However, the treatment of cluster size distributions of the present model has novel and less trivial aspects. It will confirm the above results and provide cluster length distributions that remarkably differ from those related systems and that, as far as we know, were not previously obtained in other systems with logarithmic coarsening.

The rest of this paper is organized as follows. In Sec. II we use scaling arguments to predict the logarithmic coarsening and the glassy behavior and confirm these results with numerical simulations. In Sec. III we solve the master equation within an independent interval approximation, providing the cluster length distributions. In Sec. IV we summarize our results and conclusions.

## II. SCALING OF CLUSTER LENGTH AND GLASSY BEHAVIOR

Scaling arguments can be used to predict the slow coarsening of this model, following the same lines of Ref. [16], which were previously applied to magnetic systems [17, 18] and to related non-equilibrium models [14, 15]. For simplicity, we refer to the average cluster mass as  $m$ .

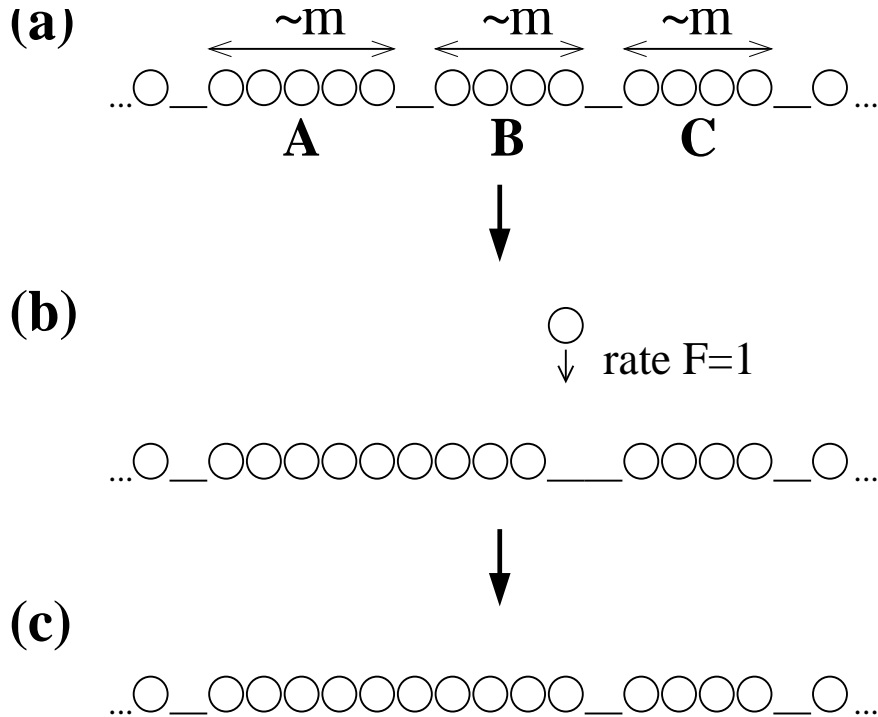


FIG. 2: Illustration of the coarsening dynamics for the construction of the scaling theory: (a) three typical neighboring clusters are shown, with lengths of the order of the average cluster size  $m$ ; (b) cluster  $B$  moves to the left, forming a larger cluster after aggregation to cluster  $A$ , and a new particle is deposited at one of the sites of the double vacancy between  $A + B$  and  $C$ ; (c) the final configuration after the deposition of a new particle at the left site of the double vacancy.

In Fig. 2a, we show a configuration with clusters of lengths typically of order  $m$ , named  $A$ ,  $B$  and  $C$ , with single empty sites between them. The time necessary for cluster  $B$  to move is of order  $\Delta t = \exp(m^\gamma/T)$ . If it moves to the left (Fig. 2b), then clusters  $A$  and  $B$  coalesce. Since the diffusion rates of clusters  $A + B$  and  $C$  are very small for large  $m$ , while the deposition rate is  $F = 1$ , a new particle will immediately be deposited in one of the sites of the double vacancy (Fig. 2b). One possible configuration after the deposition of a new particle is shown in Fig. 2c. From the initial to the final configuration (Fig. 2a to Fig. 2c), the average cluster length increase was of order  $m$ . Thus we obtain

$$\frac{dm}{dt} \sim \frac{\Delta m}{\Delta t} \sim \frac{m}{\exp(m^\gamma/T)}. \quad (1)$$

We will be mainly interested in the long-time regime in which cluster diffusion is sufficiently slow, even for small  $\gamma$ . In this case, the exponential factor at the right-hand side of Eq. (1) is much larger than  $m$ , which may be neglected at first approximation. Thus,

integrating Eq. (1), we are led to the scaling of the average cluster length as

$$m \sim (T \ln t)^{1/\gamma}. \quad (2)$$

The leading correction due to the neglected term in Eq. (1) is proportional to  $\ln(\ln t)/(\ln t)^{1-1/\gamma}$ . However, it is not expected to be the true leading correction to the dominant scaling of the model because Eq. (1) is itself an approximation, which omitted further corrections.

Numerical simulations of this model confirm the logarithmic coarsening. In Fig. 3 we show the time evolution of the average cluster length for three sets of values of  $\gamma$  and  $T$ , in which that scaling is observed in up to 7 decades of time. The data for  $\gamma = 1$ , with  $T = 1$  and  $T = 2$ , are averages over  $3 \times 10^4$  different realizations in lattices of length  $L = 10^4$ . The data for  $\gamma = 0.5$ , in which much larger clusters appear at small times, are averages over 200 realizations in lattices with  $L = 5 \times 10^4$ , up to time  $t = 10^5$ .

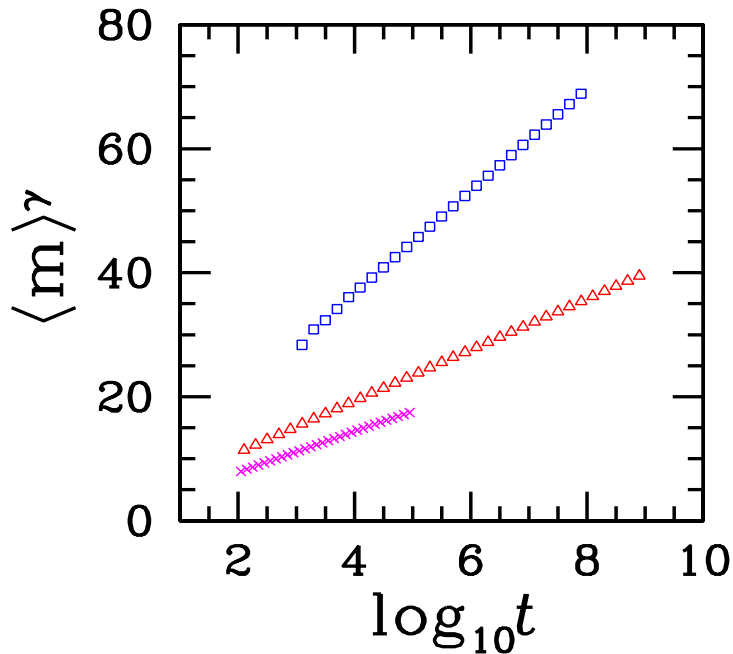


FIG. 3:  $\langle m \rangle^\gamma$  versus  $\log(t)$  for:  $\gamma = 1$  and  $T = 1$  (squares);  $\gamma = 1$  and  $T = 2$  (triangles);  $\gamma = 0.5$  and  $T = 1$  (crosses).

In Fig. 4 we show the data for the same values of  $T$  and  $\gamma$  scaled in the form  $\langle m \rangle / (T \ln t)^{1/\gamma}$

versus  $1/\ln t$ . As  $t \rightarrow \infty$  ( $1/\ln t \rightarrow 0$ ), Fig. 4 suggests an universal amplitude in the scaling relation (2), although corrections to the dominant scaling clearly depend on  $\gamma$  and  $T$ .

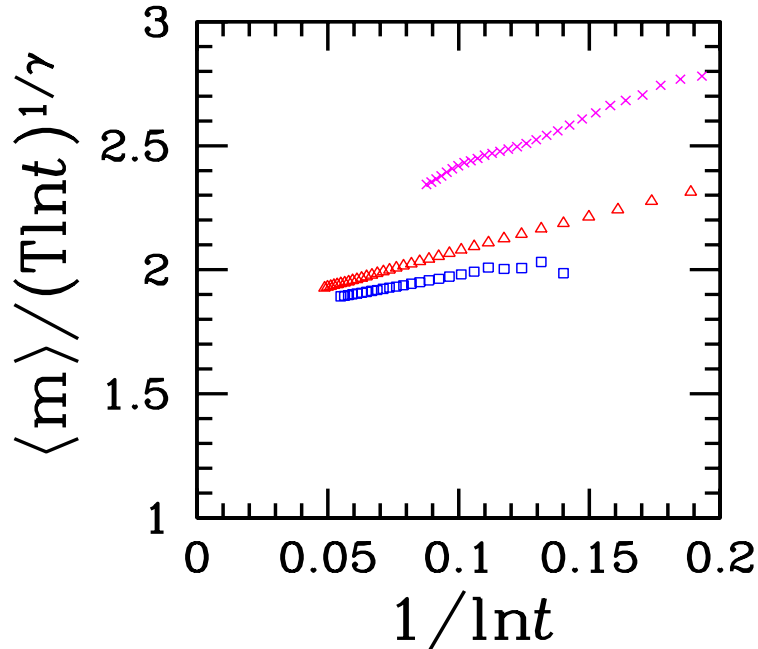


FIG. 4: Scaled average cluster size as a function of inverse of  $\ln t$  for:  $\gamma = 1$  and  $T = 1$  (squares);  $\gamma = 1$  and  $T = 2$  (triangles);  $\gamma = 0.5$  and  $T = 1$  (crosses).

The logarithmic coarsening leads to a time evolution of the density with a logarithmic correction,  $\rho = 1 - 1/(T \ln t)^{1/\gamma}$ . This type of time-dependence was also found in experiments of compaction of granular systems [19] and theoretical models to describe them [20, 21], but temperature played no role there.

Another remarkable feature of this system seen in simulations is the absence of clusters whose reduced lengths

$$y \equiv m/(T \ln t)^{1/\gamma} \quad (3)$$

are smaller than the most probable value  $y = a$  ( $a \rightarrow \text{const}$  for large  $t$ ). In order to understand this feature, consider a set of clusters with reduced size  $y = a - \epsilon$ , with any  $\epsilon > 0$ , whose diffusion rate is  $t^{(a-\epsilon)\gamma}$ . This value is larger than the diffusion rate of the clusters with  $y = a$  by a factor  $t^{\epsilon\gamma/a}$ . Thus, at large  $t$ , compared to the most probable

clusters, the clusters with  $y = a - \epsilon$  are much more mobile and are present in smaller number in the line. So they will merge into the slower larger neighboring clusters almost instantaneously within the typical time scale for diffusion of the most probable clusters (length  $y = a$ ), which causes the removal of clusters with  $y = a - \epsilon$ .

This is consistent with the simulation results shown in Fig. 5, in which we plotted the reduced probability of cluster length  $m$ ,  $(T \ln t)^{1/\gamma} P(m)$ , as a function of the reduced length  $y$ , for  $\gamma = 1$  (two temperatures in the main plot) and  $\gamma = 0.5$  (in the inset). Below a certain value  $y = a \approx 1$ , the corresponding probabilities rapidly decrease to zero and the cluster size distribution is asymptotically discontinuous at that point. A discontinuity in the slope of the distribution at  $y \approx 2a$  is also suggested in Fig. 5 and will be rigorously justified in Sec. III. Further slope discontinuities will be predicted, but they are not so clear in Fig. 5 due to the larger fluctuations in the data for large  $y$ .

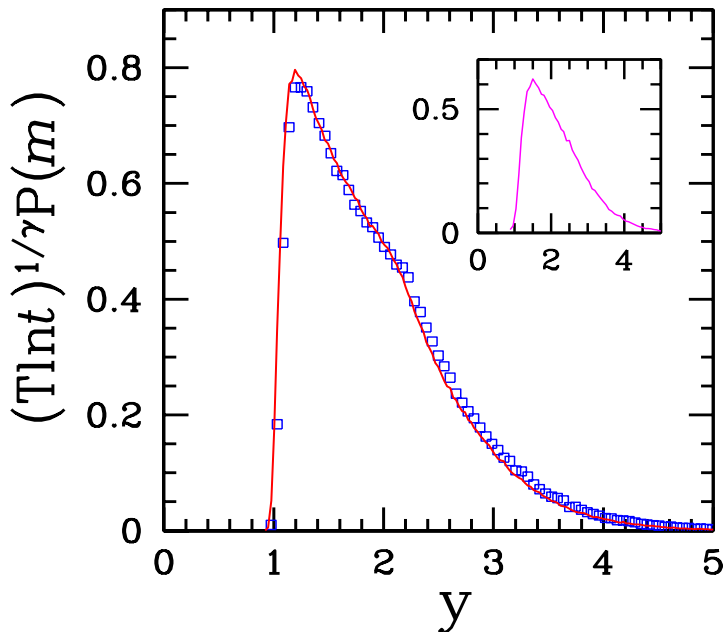


FIG. 5: Scaled probability of clusters of length (mass)  $m$  as a function of the scaled length  $y$  for  $\gamma = 1$ , with  $T = 1$  (solid curve) and  $T = 2$  (squares), at  $t = 10^8$ . The inset shows the same quantities for  $\gamma = 0.5$  and  $T = 1$ , at  $t = 10^7$  (not shown in the main plot to avoid superposition of many data points).

From the above results, the characteristic time for clusters of a given mass  $m$  to be completely eliminated from the system is  $t = \exp [(m/a)^\gamma/T]$ . The connection of the glassy behaviour to the thermally activated diffusion of microscopic structures is clear, in contrast to other kinetically constrained models whose dynamic rules are determined by the statistical equilibrium of the system.

### III. ANALYTICAL SOLUTION

Now we turn to the analysis of the model starting from a version of the master equation, following the same lines as in the solution of related models in Refs. [14] and [15].

In our original problem, each site on the line is occupied by one or zero particles, but we are interested in the evolution of cluster length. Thus, the analysis of a master equation is more easily set up by reformulating the process using a column picture, in which a column of height  $m$  represents a cluster of size  $m$  together with its adjacent vacancy on the right. This mapping is illustrated in Fig. 6.

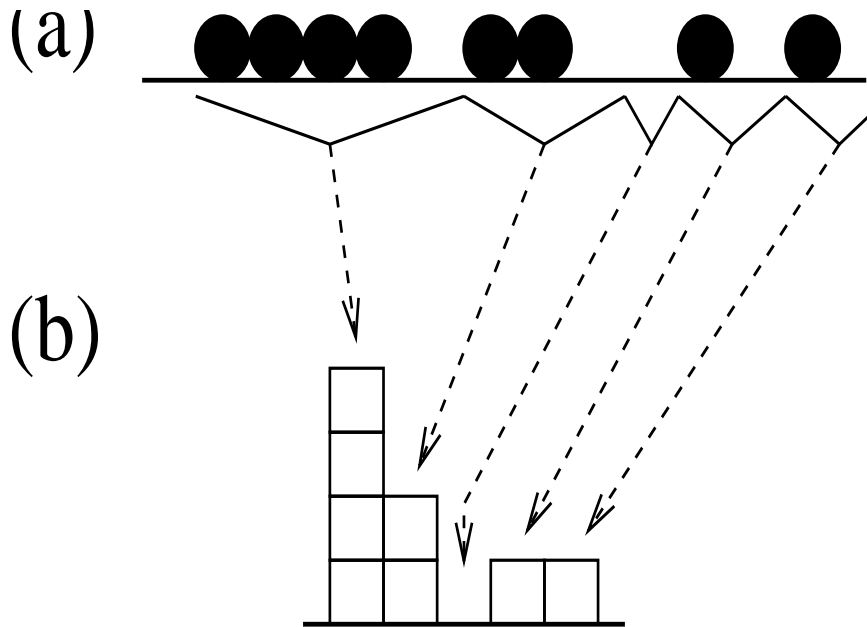


FIG. 6: Example of particle-hole configuration on a line (a) and the map (dashed arrows) into a column problem (b). Each cluster and the vacancy at its right side in (a) correspond to a column in (b) with the same mass.

Fig. 6 clearly shows that the lattice length  $L_0$  in the column picture is smaller than the

length  $L$  in the original problem (particle picture):  $L_0 = L - M$ , where  $M$  is the total mass, for periodic boundaries. As time increases and new particles are deposited,  $L_0$  decreases. However, new particles are deposited only at double vacancies of the particle picture (Fig. 1b) and the latter correspond to single vacancies in the column picture (Fig. 6). Thus, the decrease of  $L_0$  (or mass increase) is related to the probability  $P_t(0)$  of an empty site in the column problem as  $\frac{L_0(t+1)-L_0(t)}{L_0(t)} = -P_t(0) [2 - P_t(0)]$ .

The probability  $P_t(m)$  that a randomly chosen cluster in the column picture has size  $m$  at time  $t$  is given in terms of the clusters numbers,  $N(m, t)$ , by  $P_t(m) = \frac{N(m, t)}{L_0(t)}$ . The gain/loss from in/out processes provides a master equation for clusters numbers as

$$N(m, t + 1) - N(m, t) = L_0 (\mathcal{B}_m + E_m), \quad (4)$$

where  $\mathcal{B}_m$  comes from the deposition processes and  $E_m$  comes from diffusion of clusters or isolated particles. It can be rewritten in terms of cluster length probabilities as

$$(1 - P_t(0))^2 P_{t+1}(m) - P_t(m) = \mathcal{B}_m + E_m, \quad (5)$$

which allows for the changes in  $L_0$ .

In an independent interval approximation (IIA) in which joint probabilities are factorized, the contribution from deposition is given by

$$\mathcal{B}_m = P_t(0) [2\theta(m-2)P_t(m-1) - 2\theta(m-1)P_t(m) + \delta_{m,1}P_t(0) - 2\delta_{m,0}]. \quad (6)$$

Here, the factor  $P_t(0)$  accounts for the fact that deposition is allowed only at single vacancies in the column picture (Fig. 6). The first term inside brackets gives the rate of production of clusters of size  $m$  from deposition at one of the sides of a cluster of size  $m-1$ , for  $m \geq 2$ , while the third term gives the rate of production of a cluster with  $m=1$  in a double vacancy (triple vacancy in the particle picture, with the new particle being deposited at the central site). The second term corresponds to the loss of a cluster of mass  $m$  due to deposition at one of its sides and the last term the loss of vacancies due to deposition at one of the two corresponding sites in the particle picture.

The contribution from diffusion in Eq. (5) is given by

$$E_m = \sum_{r=1}^m f(r)P_t(r)P_t(m-r) + \delta_{m,0} \sum_{r=1}^{\infty} f(r)P_t(r) - \theta(m-1)f(m)P_t(m) - P_t(m) \sum_{r=1}^{\infty} f(r)P_t(r). \quad (7)$$

In Eq. (7), the function  $f(m) \equiv \exp[-(m-1)^\gamma/T]$  gives the diffusion rate for a cluster of mass  $m$ . The first term in Eq. (7) gives the rate of production of a cluster of mass  $m$  due to the coalescence of smaller clusters after diffusion of one of them. The second term corresponds to the creation of a single vacancy (double vacancy in the particle picture) due to cluster diffusion - see Fig. 1a. The loss terms correspond to coalescence of a cluster of mass  $m$  and a neighboring cluster: the third one accounts for diffusion of the cluster of mass  $m$  and the fourth one accounts for diffusion of the neighboring clusters.

In the scaling limit of large  $t$  and large  $m$  (coarsening), the probability  $P_t(m)$  must have the form

$$P_t(m) = \frac{1}{L(t)}g(y) \quad , \quad y \equiv \frac{m}{L(t)}, \quad (8)$$

with some function  $L(t)$  characterizing the growing typical cluster size.

Figs. 2a-c show that the survival time of a double vacancy is of order  $1/F = 1$ , while a typical cluster move occurs on a much larger timescale, of order  $\exp(m^\gamma/T)$ . Consequently, the onset of a double vacancy (in the particle picture) is a rare event. Nevertheless, since the double vacancy mediates deposition, its probability is required in the equation for the one-variable scaling function  $g$ , and the same scaling arguments of Sec. II lead to the expected scaling of the double vacancy probability in the particle picture as  $P_t(0) = (C/2)/t$  (see e.g. Ref. [15]).

Thus we obtain an equation for the scaling function as

$$-\frac{L'}{L} \left[ g + y \frac{dg}{dy} \right] - \frac{Cg}{t} = -\frac{C\delta(y)}{t} - h(y) - g(y)I(\infty) + \delta(y)I(\infty) + \int_0^y dy' g(y-y') h(y'), \quad (9)$$

where  $h(y) = g(y) \exp[-(Ly)^\gamma/T]$  and  $I(\infty) = \int_0^\infty dy' g(y') \exp[-(Ly')^\gamma/T]$ . The first term on the left-hand side (LHS) of Eq. (9) follows from those in Eq. (5) in the long time, continuous limit. The second term on the LHS and the first one on the right-hand side (RHS) correspond to deposition (Eq. 6) and the other terms on the RHS correspond to cluster diffusion (Eq. 7).

Eq. (9) and the corresponding equation for the generating function contrast to those of the models of Refs. [14] and [15] because a simple power-counting in Eq. (9) is not enough to provide the scaling of the average cluster size here. From the structure of Eq. (9) and the forms of  $h(y)$  and  $I(\infty)$ , we expect that the balance of dominant terms will be possible

if

$$\frac{L'}{L} = \exp[-[L(t)a]^\gamma/T]\alpha(L(t)), \quad (10)$$

where  $a$  is some constant (see below) and the function  $\alpha$  accounts for possible power-law subdominant factors. Notice also that the dominant factors of Eq. (10) are the same as those of Eq. (1), obtained from simple scaling arguments.

As  $t \rightarrow \infty$ , we expect  $L(t) \rightarrow \infty$ , but the last term in the RHS of Eq. (9) will provide a divergent contribution for  $y' < a$ . This contribution is not balanced out by other terms unless  $g(y) = 0$  for  $y < a$ . With this assumption, we obtain a dominant term on the LHS of Eq. (9) with a factor  $e^{-(La)^\gamma/T}$  and, in the integral at the RHS, a factor  $e^{-(Ly')^\gamma/T}$ , which provides a dominant cancelling term for  $y \geq a$ .

The solution of Eq. (10) is exactly the logarithmic growth of  $L(t)$  obtained from scaling arguments (Eq. 2), thus providing the expected scaling of average cluster length. The above assumption for the function  $g$  confirms, within the IIA, the elimination of all clusters with masses smaller than  $aL(t) \sim (T \ln t)^{1/\gamma}$ .

The scaling function has the form

$$g(y) = \theta(y - a) g_1(y), \quad (11)$$

which leads to an equation for the function  $g_1(y)$  as

$$g_1 + y \frac{dg_1}{dy} + C g_1 - C \delta(y) = \frac{a g_1(a)}{k} [g_1 \theta(y - a) - g_1(y - a) \theta(y - 2a) + \delta(y - a) - \delta(y)], \quad (12)$$

where  $k$  is constant. Consequently, a discontinuity in the slope of  $g(y)$  is obtained at  $y = 2a$ . Subsequently, further discontinuities appear at  $y = 3a$ ,  $y = 4a$  and so on. The function  $g$  can be shown to be continuous except at  $y = a$ , where the discontinuity implies  $k = 1$  in Eq. (12). These findings agree with those in Fig. 5, in which the probabilities of cluster lengths with  $y < a \sim 1$  tend to zero asymptotically and the slope of the scaled probability clearly changes at  $y \approx 2a$ .

From Eq. (12) we obtain the distribution for  $a < x < 2a$  as

$$g(y) = A y^{[ag(a)-(C+1)]}, \quad (13)$$

where  $A$  is a constant. In Fig. 7 we show  $\log P(m)$  versus  $\log y$  for  $\gamma = 1$  and  $T = 1$ , at time  $t = 10^8$ , with a linear fit that confirms the power-law decay predicted in Eq. (13). Notice that, although the scaling arguments of Sec. II were capable of predicting several features of

the model, the analytical solution of the master equation, even within the IIA, is essential to predict the shape of the scaled cluster size distribution.

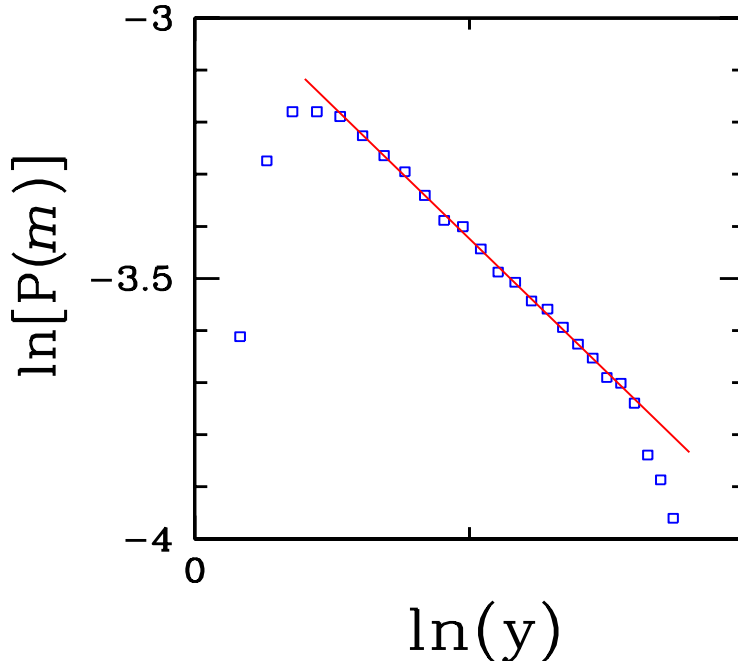


FIG. 7:  $\ln [P(m)]$  versus  $\ln (y)$  for  $\gamma = 1$  and  $T = 1$ , at  $t = 10^8$ , and a linear fit of the data in the region  $1.4 \leq y \leq 2.2$ .

For  $2a < y < 3a$ , the distribution is  $g(y) = By^{[ag(a)-(C+1)]} - A(y - a)^{[ag(a)-(C+1)]}$ , but the low accuracy of our data in that region does not allow a reliable test of this form.

#### IV. CONCLUSION

We presented a one-dimensional model of polymer growth and diffusion with frustration mechanisms for density increase and with diffusion rates of Arrhenius form, with mass-dependent energy barriers. The non-universal logarithmic coarsening involves the exponent  $\gamma$  and can be predicted by scaling arguments. The model also shows strong glass behavior of the characteristic times for elimination of all polymers up to a given length. These features are confirmed by the solution of the master equation within an independent interval approximation (IIA). This solution also provides the distribution of cluster sizes, which shows

discontinuities at a sequence of points and a power-law decay for sizes near the most probable one. These findings are confirmed by numerical simulations with good accuracy.

The logarithmic coarsening and Arrhenius-type behavior were also obtained in other systems, but our model presented a different scenario for the onset of these properties, in which there is no reference to equilibrium states. Instead, all these features are obtained during the non-equilibrium system evolution assuming a thermal contact between the clusters and their surroundings at a temperature  $T$ , but not an approach to an equilibrium macroscopic state with that temperature.

The elimination of clusters with lengths below a certain threshold is also present in the paste-all model of Derrida et al [22], although that is a direct consequence of the model prescription, namely the elimination of the smallest cluster of the system at any time. Instead, in the present model that elimination is obtained only in the scaling limit (long times, large clusters), in which diffusion coefficients of small clusters become infinitely larger than those of large clusters. The same type of distribution appears in the East model [9, 10], in which the rules for spin flips are asymmetric (an artificial but essential ingredient for obtaining slow dynamics there). On the other hand, a power-law coarsening and fragile glass behavior are obtained in the East model, which contrasts to our findings.

The successful application of the IIA for the present problem and for previous models with particle detachment from clusters [14, 15] also deserves some comments. In these models, the coarsening arises from coalescence of clusters and the reverse process is increasingly improbable (altogether improbable in the present case). Since the initial state is without cluster-cluster correlations, no correlations between the masses/lengths of neighbouring clusters can build up, so the IIA becomes exact in the late coarsening limit. This interpretation is corroborated by the successful comparison of IIA predictions and simulation results. It seems that IIA fails only when we focus on rare processes which occur in narrow time windows in which the system is dominated by reversible and highly correlated processes [15], which is not the case in the present model.

## Acknowledgments

FDAA Reis thanks the Rudolf Peierls Centre for Theoretical Physics of Oxford University, where part of this work was done, for the hospitality, and acknowledges support by CNPq

and FAPERJ (Brazilian agencies).

RB Stinchcombe acknowledges support from the EPSRC under the Oxford Condensed Matter Theory Grants, numbers GR/R83712/01 and GR/M04426.

- 
- [1] F. Ritort and P. Sollich, *Adv. Phys.* **52**, 219 (2003).
  - [2] L. F. Cugliandolo, *cond/mat/0210312* (2002).
  - [3] G. H. Fredrickson and H. C. Andersen, *Phys. Rev. Lett.* **53**, 1244 (1984); *J. Chem. Phys.* **83**, 5822 (1985).
  - [4] A. Crisanti, F. Ritort, A. Rocco, and M. Sellitto, *J. Chem. Phys.* **113**, 10615 (2000).
  - [5] W. Kob and H. C. Andersen, *Phys. Rev. E* **48**, 4364 (1993).
  - [6] C. Toninelli, G. Biroli, and D. S. Fisher, *Phys. Rev. Lett.* **92**, 185504 (2004); *cond-mat/0410647* (2004).
  - [7] J. P. Garrahan, *J. Phys. Cond. Matt.* **14**, 1571 (2002).
  - [8] A. C. Pan, J. P. Garrahan, and D. Chandler, *cond-mat/0410525* (2004).
  - [9] J. Jäckle and S. Eisinger, *Z. Phys. B* **84**, 115 (1991).
  - [10] P. Sollich and M. R. Evans, *Phys. Rev. Lett.* **83**, 3238 (1999).
  - [11] K. R. Paserba and A. J. Gellman, *Phys. Rev. Lett.* **86**, 4338 (2001).
  - [12] A. R. C. Baljon, M. H. M. Van Weert, R. B. DeGraaff, and R. Khare, *cond-mat/0408523* (2004).
  - [13] E. R. Weeks, J. C. Crocker, A. C. Levitt, A. Schofield, and D. A. Weitz, *Science* **287**, 627 (2000).
  - [14] F. D. A. Aarão Reis and R. B. Stinchcombe, *Phys. Rev. E* **70**, 036109 (2004).
  - [15] F. D. A. Aarão Reis and R. B. Stinchcombe, *Phys. Rev. E* **71** 026110 (2005).
  - [16] M. R. Evans, *J.Phys:Condens. Matter* **14** 1397 (2002).
  - [17] Z. W. Lai, G. F. Mazenko, and O. T. Valls, *Phys. Rev. B* **37**, 9481 (1988).
  - [18] J. D. Shore, M. Holzer, and J. P. Sethna, *Phys. Rev. B* **46**, 11376 (1992).
  - [19] J. B. Knight, C. G. Fandrich, C. N. Lau, H. M. Jaeger, and S. R. Nagel, *Phys. Rev. E* **51**, 3957 (1995).
  - [20] R. B. Stinchcombe and M. Depken, *Phys. Rev. Lett.* **88**, 125701 (2002).
  - [21] A. Lefèvre, L. Berthier, and R. B. Stinchcombe, *Phys. Rev. E* **72**, 010301 (2005).

[22] B. Derrida, C. Godrèche, and I. Yekutieli, Phys. Rev. A **44**, 6241 (1991).